Computational Algorithms and Numerical Dimensions

www.journal-cand.com

Com. Alg. Num. Dim Vol. 2, No. 1 (2023) 35–46.

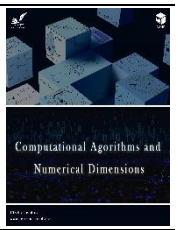

Paper Type: Original Article

A Local Meshless Radial Basis Functions Based Method for Solving Fractional Integral Equations

Mehdi Radmanesh[1], Mohammad Javad Ebadi[2,3,*]

[1] Department of Mathematics, Graduate University of Advanced Technology of Kerman, Kerman, Iran; m.radmenesh@gmail.com.
[2] Section of Mathematics, International Telematic University Uninettuno, Corso Vittorio Emanuele II, 39, 00186 Roma, Italy; ebadi2020@gmail.com.
[3] Department of Mathematics, Chabahar Maritime University, Chabahar, Iran; ebadi2020@gmail.com.

Citation:

Radmanesh, M., & Ebadi, M. J. (2023). A local meshless radial basis functions based method for solving fractional integral equations. *Computational algorithms and numerical dimensions, 2*(1), 35-46.

Received: 10/09/2022 Reviewed: 12/10/2022 Revised: 09/11/2022 Accepted: 20/12/2022

Abstract

This paper presents a Localized Radial Basis Functions Collocation Method (LRBFCM) for numerically solving one and 2-dimensional Fractional Integral Equations (2D-FIEs). The LRBFCM approach decomposes the main problem into several local sub-problems of small sizes, effectively reducing the ill-conditioning of the overall problem. By employing the collocation approach and utilizing the strong form of the equation, the proposed method achieves efficiency. Additionally, the matrix operations only require the inversion of small-sized matrices, further contributing to the method's efficiency. To demonstrate the effectiveness of the LRBFCM, the paper provides test problems encompassing linear, nonlinear, Volterra, and Fredholm types of Fractional Integral Equations (FIEs). The numerical results showcase the efficiency of the proposed method, validating its performance in solving various types of FIEs.

Keywords: Fractional calculus, Local meshless methods, Fractional integral equations, Collocation methods.

1 | Introduction

In recent years, fractional calculus has gained significant attention for its ability to model complex phenomena in various fields such as physics, engineering, and finance [1]–[10], [11]–[13]. Fractional Integral Equations (FIEs), a vital component of fractional calculus, have been extensively studied and applied in numerous applications. To solve these equations, several numerical methods have been proposed, including finite difference methods [14], finite element methods [15], and spectral methods [16]. Among these methods, meshless methods have emerged as a promising alternative due to their flexibility and adaptability in handling irregular geometries and complex boundary conditions [17]. Radial Basis Functions (RBFs) are a popular choice for meshless methods as they provide a simple and efficient way to approximate functions in high-dimensional spaces [18]. RBF-based methods have been successfully applied to solve various types of integral equations, including Fredholm and Volterra integral equations [19]. However, the application of RBFs to FIEs is still relatively limited. Recent attempts have been made to develop RBF-based methods for solving FIEs. For example, Dehghan and Mirzaei [20] proposed a meshless method based on RBFs for solving Fractional

Corresponding Author: ebadi2020@gmail.com
https://doi.org/10.22105/cand.2023.400616.1064

Fredholm Integral Equations (FFIEs), and Wang et al. [21] developed a similar approach for Fractional Volterra Integral Equations (FVIEs). These methods have demonstrated promising results in terms of accuracy and computational efficiency. Nevertheless, there is still room for improvement in the development of RBF-based methods for FIEs, particularly in the investigation of local RBF methods that focus on small subsets of the problem domain [22]. Meshless methods have garnered attention due to their straightforward numerical implementation without the need for meshing or re-meshing. These methods offer flexibility in handling irregular geometries and can be easily extended to higher-dimensional problems. They can employ strong form [23]–[26] or weak form formulations of the governing equations [27]–[31]. Local methods have been proposed to address the fully assembled and ill-conditioned final matrices obtained by global methods. Popular local methods include the Local Multi-Quadric (LMQ) approximation method [32]–[34] and the Finite Collocation (FC) approach [35], [36] which reduce the problem into local sub-problems and assemble them into a sparse final global matrix. In this paper, we propose a Local Radial Basis Functions (LRBF) method for numerically solving FIEs. Our approach combines the advantages of RBFs and local methods, providing a flexible and efficient framework for solving a wide range of FIEs. We present a detailed analysis of the proposed method, including convergence properties and error estimates, along with numerical examples to demonstrate its effectiveness and robustness. The remainder of the paper is organized as follows: Section 2 presents basic definitions in FIEs and fractional calculus necessary for the subsequent sections. In Section 3, we describe the method of local RBF for discretization of FIEs. Numerical results are presented in Section 4. Finally, Section 5 provides a summary of the paper.

2 | Fractional Integral Equations

The basic definitions for the Riemann-Liouville Fractional Calculus (RLFC) [1], [37] are presented in this section.

Definition 1 ([37]). Let a finite interval j=[a, b](-∞<a<b<∞)of $\Re$. The left and right Riemann-Liouville Fractional Integrals (RLFIs) ${}_aI_t^{-\alpha}f$ and ${}_tI_b^{-\alpha}f$ of order $\alpha \in \Re^+$ are given respectively as below:

$$ {}_a\mathrm{I}_t^{-\alpha}\mathrm{f}(t)=\frac{1}{\Gamma(\alpha)}\int_a^t(t-x)^{\alpha-1}\mathrm{f}(x)dx,\quad (t>a,\alpha>0), \tag{1}$$

and

$$ {}_a\mathrm{I}_t^{-\alpha}\mathrm{f}(t)=\frac{1}{\Gamma(\alpha)}\int_t^b(x-t)^{\alpha-1}\mathrm{f}(x)dx,\quad (t>a,\alpha>0), \tag{2}$$

where Γ(α) is known as gamma function. In the special case of $\alpha = n \in N^+$, *Eqs. (1)* and *(2)* are the nth integrals in the following forms:

$$ {}_a\mathrm{I}_t^{-n}\mathrm{f}(t)=\frac{1}{(n-1)!}\int_a^t(t-x)^{n-1}\mathrm{f}(x)dx, \tag{3}$$

and

$$ {}_t\mathrm{I}_b^{-n}\mathrm{f}(t)=\frac{1}{(n-1)!}\int_t^b(x-t)^{n-1}\mathrm{f}(x)dx. \tag{4}$$

Similarly, the below definition for the two dimensional RLFIs of order r is given by considering $L^1(J)$ as the space of Lebesgue-integrable functions $\omega : J \to \mathbb{R}^n$ with the following norm:

$$\| \mathrm{w} \|_{L^1}=\int_0^a\int_0^b\| \mathrm{w}(x,y)\| dydx,$$

where J = [0, a]×[0, b].

Definition 2 ([37]). The left-sided mixed RLFI of order r = (r_1, r_2) of the function u(x, y) is defined as

Radmanesh and Ebadi| Com. Alg. Num. Dim. 2(1) (2023) 35-46

$$I_{\Theta}^{r}u)\ x,y) = \frac{1}{\Gamma(r_1)\Gamma(r_2)}\int_0^x \int_0^y x-s)^{r_1-1}\ y-t)^{r_2-1}u\ s,t)dtds, \tag{5}$$

where u ϵ L^1 J). r ϵ $(0,\infty)\times\ 0,\infty)$ and $\Theta = (0, 0)$. So, we have

I. $(I_{\Theta}^{\Theta}u)\ x,y) = u\ x,y).$

II. $(I_{\Theta}^{\tau}u)\ x,y) = \int_0^x \int_0^y u\ x,y)dtds$ *where* $\tau = 1,1)$ *and for all* $x,y) \in J.$

III. $(I_{\Theta}^{r}u)\ x,0) = I_{\Theta}^{r}u)\ 0,y) = 0$ *for* $x \in [0,a],\ y \in [0,b].$

IV. Let $\lambda, \omega \in -1,\infty)$ *then* $\left(I_{\Theta}^{r}\ x^{\lambda}y^{\omega}\right) = \frac{\Gamma\ \lambda+1)\Gamma\ \omega+1)}{\Gamma\ \lambda+r_1+1)\Gamma\ \omega+r_2+1)}x^{\lambda+r_1}y^{\omega+r_2}$ *for all* $x,y) \in J.$

The interested reader can refer to [38] for more details of the left-sided mixed RLFI. The following is the FVIE:

$$u(x) = f\ x) + \frac{1}{\Gamma(\alpha)}\int_0^x K\ x,t)\ x-t)^{\alpha-1}u\ t)dt, \qquad 0 \le x \le 1, \tag{6}$$

where $\alpha > 0$ is a real number, the right-side function f is given, and K(x, t) is the kernel. $\alpha = 1$ is corresponding to the ordinary (non-fractional) Volterra equation. Note that when α is non-integer, the term $(x-t)^{\alpha}$ adds only up for $x \ge t$. Hence, defining the FFIE as the following form is reasonable:

$$u\ x) = f\ x) + \frac{1}{\Gamma(\alpha)}\left[\int_A^x K(x,t)(x-t)^{\alpha-1}u\ t)dt + \int_x^B K\ x,t)\left(x-t)^{\alpha-1}u\ t)dt\right]. \tag{7}$$

Two-Dimensional (2D) FVIE is defined as follows:

$$u\ x) = g\ x,y) + \frac{1}{\Gamma(r_1)\Gamma(r_2)}\int_a^x \int_a^y x-s)^{r_1-1}\ y-t)^{r_2-1}K\left(x,y,s,t,u\ s,t)\right)dsdt. \tag{8}$$

3 | Discretization by LRBF

In this section, the local RBF method is used as a technique for approximation of FIEs. The function Φ: $R^+ \to R$ is RBF which is defined as the function of distance $r = \|x - x_j\|$ [39]. Our choice of RBF is the MQ $\phi(r) = \sqrt{r^2 + c^2}$ which belongs to a class of infinitely differentiable global RBFs. Consider the following VIE of fractional order:

$$u(x) = f(x) + \frac{1}{\Gamma(\alpha)}\int_0^x K(x,t)(x-t)^{\alpha-1}u(t)dt, \quad 0 \le \alpha \le 1. \tag{9}$$

A set of N distinct points $X=\{x_1, x_2, \ldots, x_N\}$ in R, which are called centers is used to discretize the domain of the problem. There are not any restrictions on the location of the centers or on the shape of domains. The solution u can be approximated at each of N centers by a localized formulation as below:

$$u\ x_s) \simeq \tilde{u}\ x_s) = \sum_{j=1}^{n} \lambda_j^s \phi\left(\|x_s - x_j^s\|_2\right), \tag{10}$$

where n is known as the number of nearest neighbouring points $\{x_j^s\}$ which surrounds the collocation point x_s, containing the collocation point itself. The stencils are center and its n-1 neighbours. λ_j 's are the unknown coefficients and ϕ is an RBF. By applying the interpolation conditions

$$u(x_i^s) \simeq \tilde{u}\ x_i^s) = \sum_{j=1}^{n} \lambda_j \phi\left(\|x_i^s - x_j^s\|_2\right) = \lambda^T\phi, \quad i = 1,2,\ldots,n. \tag{11}$$

On each N stencil we have an n×n linear system $\phi\lambda^s = u^s$. The matrix ϕ with elements $\phi_{i,j} = \phi(\|x_i^s - x_j^s\|_2)$ is called the interpolation matrix. If ϕ(x) is a positive definite RBF and all collocation points are distinct, then the interpolation matrix of RBF ϕ is non-singular and we have

$$\lambda^s = \phi^{-1} u^s, \tag{12}$$

where

$$\lambda^s = (\lambda_1^s, \lambda_2^s, \ldots, \lambda_n^s), \quad u^s = (u_1^s, u_2^s, \ldots, u_n^s).$$

Therefore, the estimated solution $\tilde{u}(x_s)$ can be approximated by the given nodal values $u(x_j^s)$ at stencil points:

$$\tilde{u}^s = \phi^s \lambda^s = \phi^s \phi^{-1} u^s = \Psi u^s, \tag{13}$$

where $\boldsymbol{\phi}^s = \phi(\|x_s - x_j^s\|_2)$. If we rewrite *Eq. (13)* in the approximate solution terms $\tilde{u}(x_j)$ at all collocation points, then

$$\tilde{u}(x_s) = \Psi u,$$

where Ψ is a sparse matrix of order N×N which has at most n×N nonzero elements. Considering *Eq. (6)* and Legendre-Gauss-Lobatto nodes and weights, we have

$$\Psi u = f(x_j) + \frac{1}{\Gamma(\alpha)} \sum_{k=1}^{m} \omega_k (x_j - t_k)^{\alpha-1} K(x_j, t_k) u^T \Phi(t_k), \quad j = 1,2,\ldots,N, \quad i = 1,2,\ldots,n, \tag{14}$$

where w_k and t_k for k =1, 2, ..., m are Legendre-Gauss-Lobatto weights and nodes, respectively. Thus, we have

$$A\tilde{u} = B. \tag{15}$$

As a system of linear sparse equations. The approximate solutions at all collocation points can be found by solving *Eq. (15)*. In the same manner, for 2D-FIE we have

$$u\ p) \simeq \sum c_\gamma\, \phi(\|p - p_\gamma\|) = C^T \varphi\ p) \Rightarrow \quad C = \varphi^{-1} u, \tag{16}$$

where p=(x, y) and $p_\gamma = (x_\gamma, y_\gamma) \in R^2$. We can remove the dependence on the RBF expansion coefficients from *Eq. (16)* by the following:

$$u(p_s) \simeq \sum c_\gamma\, \phi(\|p_s - p_\gamma^s\|) = \phi^s C^s = \phi^s \phi^{-1} u^s = \Psi u^s. \tag{17}$$

Substituting *Eqs. (16)* and *(17)* in *Eq. (9)*, we have

$$\Psi u^s = g\ x, y) + \frac{1}{\Gamma\ r_1)\Gamma\ r_2)} \int_a^x \int_a^y x - s)^{r_1 - 1}\ y - t)^{r_2 - 1} K(x, y, s, t, \phi^{-1}\phi\ s, t)\tilde{u})\, ds\, dt. \tag{18}$$

Substituting the given collocation points into the above equation and applying Legendre quadrature integration formula, we obtain

$$\Psi\tilde{u} = g(x_i, y_j) + \frac{1}{\Gamma(r_1)\Gamma(r_2)} \sum_{k=0}^{m} \sum_{l=0}^{m} \omega_k \omega_l (x_i - \xi_k)^{r_1 - 1} (y_j - \tau_l)^{r_2 - 1} K(x_i, y_j, \xi_k, \tau_j, \phi(\xi_k, \tau_l) \Phi^{-1} \tilde{u}).$$

4 | Numerical Experiments

In this section, we apply the proposed method on some test problems and then we present the numerical results. For evaluating error estimation, the quantity M = 2J can be defined in which J is the maximal level of resolution and the interval [a, b] can be divided into 2M subintervals with the equal length, and N = 2M + 1, where N is the number of collocation point x_l. When the problem $u = u_{ex}(x)$ has a known exact solution, the differences

$$\Delta_{ex}(l) = \tilde{u}(x_l) - u_{ex}(x_l), \quad l = 1,2,\ldots,2M+1,$$

can be calculated and the error estimation can be estimated as

$$\delta_{ex} = \max_l |\Delta_{ex}(l)|,$$

or

Radmanesh and Ebadi| Com. Alg. Num. Dim. 2(1) (2023) 35-46

$$\sigma_{ex} = \|\tilde{u} - \frac{u_{ex}\|}{2M}.$$

When the problem has unknown exact solution, the problem can be solved by some level of resolution J, and $u_J(x)$ represents the result. Then, these calculations are repeated for J+1 getting $u_{J+1}(x)$. The differences

$$\Delta_J(x_l) = u_J(x_l) - u_{J+1}(x_l),$$

are defined, where x_l, l = 1, 2, ..., 2M + 1 are the collocation points at the level J. The error estimations is then obtained with

$$\delta_J = \max|\Delta_J(x_l)|, \quad \sigma_J = \|\Delta_J(x_l)\|/(2M).$$

4.1 | Test Problem 1, Abel's Integral Equation of the Second Kind

The below Abel's integral equation of the second kind is given [40].

$$u(x) = \frac{1}{1+x} + \frac{2\arcsin\left(\sqrt{x}\right)}{\sqrt{1+x}} - \int_0^x \frac{u(s)}{\sqrt{s+x}}dt, \quad 0 \le x \le 1. \tag{19}$$

Table 1. The RMS error obtained with different values of nodal N for Example 1.

	LRBF			GRBF
N	n = 6	n = 9	n = 16	
20	2.6×10^{-3}	2.2×10^{-3}	2.1×10^{-3}	2.2×10^{-3}
30	2.1×10^{-3}	2.2×10^{-3}	2.5×10^{-3}	2.3×10^{-3}
50	2.1×10^{-3}	2.4×10^{-3}	1.2×10^{-3}	2.2×10^{-3}
85	1.9×10^{-3}	3.0×10^{-3}	1.7×10^{-2}	1.6×10^{-3}

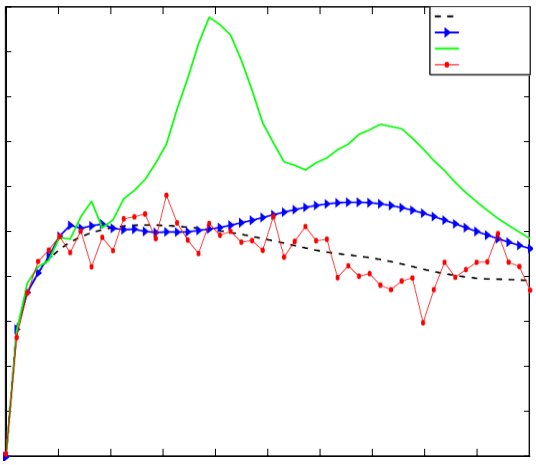

Fig. 1. RMS errors for local and global RBF methods for Example 1.

Which its exact solution is $u(x) = \frac{1}{1+x}$. Numerical results versus the numbers of nodal points and stencil are shown in *Table 1*. *Fig. 1* shows the error curves for local and global RBF methods with 50 number of nodal points. *Fig. 2* presents the RMS error with 50 nodal points and versus stencils. According to *Figs. 1* and *2*, the optimal choice of the stencil size for 50 nodal points is n = 6. The local method with $n \ll N$ is often just as accurate as the global method.

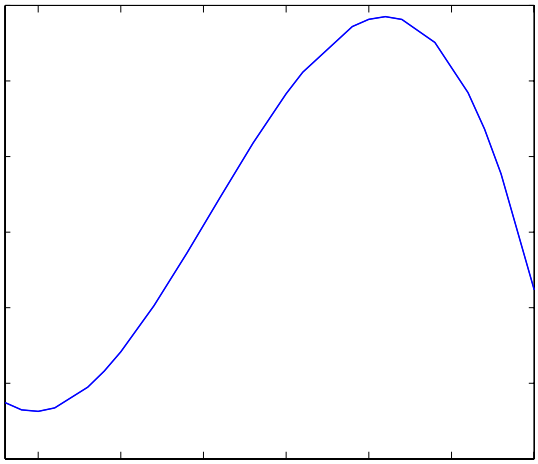

Fig. 2. RMS error for N = 50 and versus stencils for Example 1.

4.2 | Test Problem 2

Consider the equation

$$u(x)-\frac{1}{\Gamma(\alpha)}[\int_0^x(2-x-t)(x-t)^{\alpha-1}u(t)dt+\int_x^3(2-x-t)(x-t)^{\alpha-1}u(t)dt]=x^2+\frac{15}{4}.$$

When $\alpha = 1$, corresponding the non-fractional equation, $u(x) = x^2 - 3$, $x \in [0,3]$ is the exact solution. Results obtained with N = 45 nodal points and stencil size n = 15 are given in *Figs. 3* and *4* and *Table 2*. The analysis of error has been done for $\alpha = 0.9$, *Table 2* shows the results. Approximate solutions with various α are presented in *Figs. 3* and *4*. Considering the results, accuracy of the global method is more than local method, but the local method is faster. The results are the same as that of [41].

Table 2. Numerical results for Example 2 with $\alpha = 0.9$.

		LRBF		GRBF	
J	2M	δ_J	σ_J	δ_J	σ_J
3	16	0.4784	2.9×10^{-2}	0.0329	2.1×10^{-3}
4	32	0.2482	7.8×10^{-3}	0.0325	1.0×10^{-3}
5	64	0.1772	1.4×10^{-3}	0.0367	5.7×10^{-4}
6	128	0.8643	6.8×10^{-3}	0.1239	9.6×10^{-4}

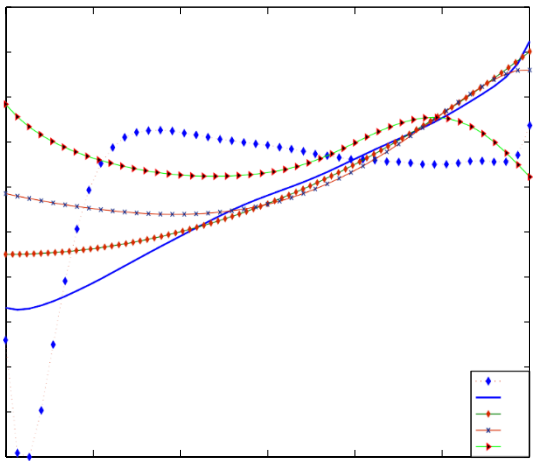

Fig. 3. Numerical solutions of Example 2 for various α.

4.3 | Test Problem 3, 2D Nonlinear FVIE

Consider the following 2D nonlinear FVIE:

$$u(x,y)-\frac{1}{\Gamma(\frac{3}{2})\Gamma(\frac{5}{2})}\left[\int_0^x\int_0^y (x-s)^{\frac{1}{2}}(y-t)^{\frac{3}{2}}\sqrt{xyt}[u(s,t)]^2\,dtds\right]=\sqrt{y}\left(\frac{-1}{180}x^3y^{\frac{7}{2}}+\sqrt{\frac{x}{3}}\right). \quad (20)$$

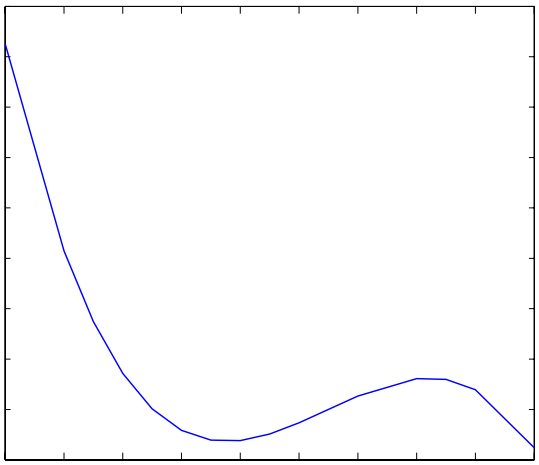

Fig. 4. RMS error versus N for Example 2.

For which the exact solution is $u(x, y) = \frac{\sqrt{3xy}}{3}$. The results with shape parameter c = 4 are presented in *Table 3*. The RMS error versus the number of the nodal points N with 3 × 3 and 5 × 5 stencils is given in *Fig. 5*. *Fig. 6* shows the error with $N= 8^2$, 3 × 3 and 5 × 5 stencils. *Figs. 7* and *8* show the cross section of the approximate solutions and errors with $N = 10^2$, 3 × 3 stencils and fixed values of y.

4.4 | Test problem 4, 2D nonlinear FFIE

Consider the following 2D nonlinear FFIE:

$$u(x,y)-\frac{1}{\Gamma(\frac{9}{2})\Gamma(\frac{3}{2})}\left[\int_0^T\int_0^T (T-s)^{\frac{7}{2}}(T-t)^{\frac{1}{2}}5\sqrt{s}(y-x)[u(s,t)]^2\,dtds\right]=f(x,y),$$

where

$$T=1,$$

$$f(x,y)=\frac{322560x^2-322349x+161069y}{322560}. \quad (21)$$

Table 1. Numerical results obtained with different number of nodal points for Example 3.

		3 × 3 Stencil	5 × 5 Stencil	
N	**δex**	**RMS**	**δex**	**RMS**
6^2	1.3×10^{-2}	5.8480×10^{-3}	8.5×10^{-2}	3.5273×10^{-3}
7^2	3.0×10^{-2}	1.2000×10^{-3}	4.6×10^{-2}	2.9653×10^{-3}
$_8 2$	1.1×10^{-2}	3.7382×10^{-4}	3.0×10^{-3}	1.0000×10^{-3}
9^2	1.8×10^{-3}	2.7669×10^{-4}	2.9×10^{-3}	9.5724×10^{-4}
10^2	2.1×10^{-4}	8.6700×10^{-5}	5.1×10^{-3}	3.3647×10^{-4}
11^2	3.7×10^{-4}	9.2053×10^{-5}	4.2×10^{-2}	3.2812×10^{-3}
12^2	7.4×10^{-3}	8.1000×10^{-4}	7.5×10^{-2}	1.4528×10^{-2}

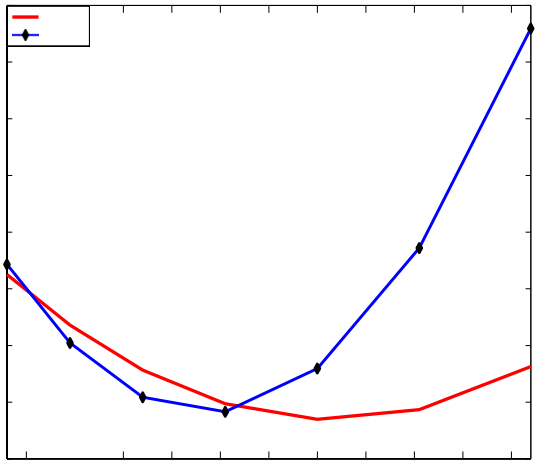

Fig. 5. RMS error versus N for Example 3 obtained with 3×3 and 5×5 sencils.

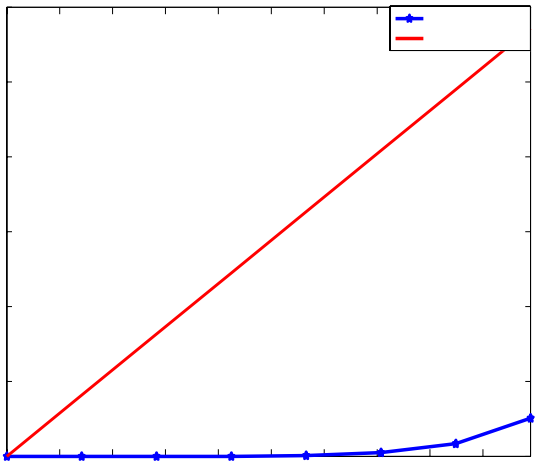

Fig. 6. RMS error obtained for Example 3.

Table 4. Numerical results obtained with different number of nodal points for Example 4.

	3 × 3 Stencil		5 × 5 Stencil	
N	δex	**RMS**	δex	**RMS**
6^2	1.2×10^{-3}	5.9600×10^{-4}	8.2×10^{-3}	8.9394×10^{-4}
7^2	1.0×10^{-3}	5.8873×10^{-4}	6.6×10^{-3}	5.6580×10^{-4}
8^2	1.0×10^{-3}	2.3020×10^{-4}	5.4×10^{-3}	3.4530×10^{-4}
9^2	6.4×10^{-4}	2.9741×10^{-5}	3.2×10^{-3}	3.0230×10^{-4}
10^2	3.4×10^{-3}	1.0102×10^{-4}	5.8×10^{-4}	2.9436×10^{-5}
11^2	4.3×10^{-3}	5.6420×10^{-4}	6.3×10^{-4}	2.3549×10^{-4}
12^2	6.3×10^{-2}	2.3751×10^{-3}	2.6×10^{-2}	1.1205×10^{-3}

And the exact solution of this equation is $u(x,y) = x^2 - x + \frac{1}{2}y$. The results with different number of nodal points are shown in *Table 4*.

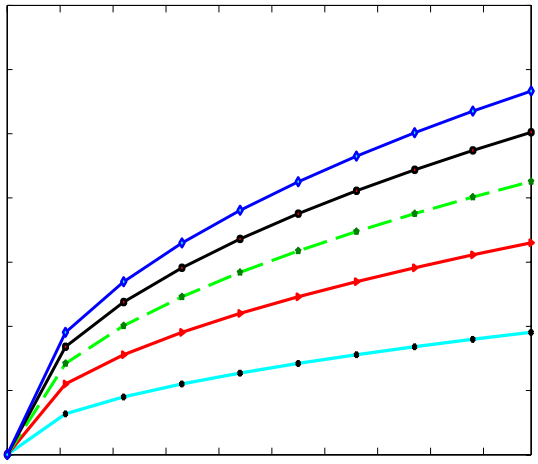

Fig. 7. Cross section of approximate solution obtained with N = 10^2 and 3×3 stencils for Example 3.

4.5 | Test Problem 5

Consider the 2D nonlinear FVIE:

$$u(x,y)-\frac{1}{\Gamma\left(\frac{4}{3}\right)\Gamma\left(\frac{2}{3}\right)}\left[\int_0^x\int_0^y (x-s)^{\frac{1}{3}}(y-t)^{\frac{1}{3}}\beta\left(\frac{4}{3},\frac{2}{3}\right)x^{\frac{4}{3}}y^{\frac{2}{3}}\left[u(s,t)\right]^2\,dtds\right]=f(x,y),$$

where

$$f(x,y)=x^2y\left(y-1-\frac{19683x^2\left(77y+18y^2\left(3y-7\right)\right)}{22422400}\right).$$

$\beta(.,.)$ denotes the two dimensional Beta function. Exact solution of this problem is $u(x, y) = x^2(y^2-y)$. *Table 5* illustrates the numerical results with different number of nodal points for this test problem. The results obtained in Test *Problems (3), (4)* and *(5)* with local RBF method are more accurate than the results obtained in [37].

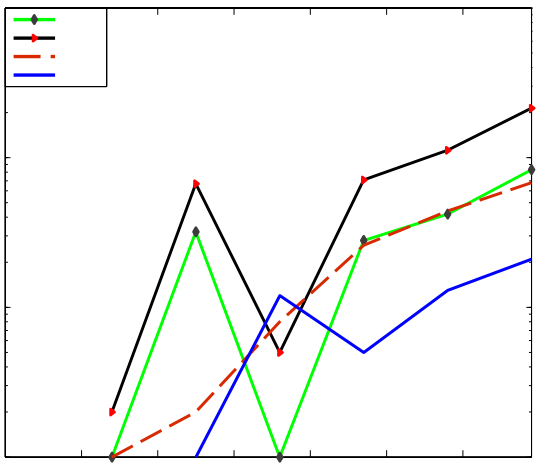

Fig. 8. Cross section of approximate solution obtained with N = 10^2 and 3×3 stencils for Example 3.

Table 5. Numerical results obtained with different number of nodal points for Example 5.

	3 × 3 Stencil		5 × 5 Stencil	
N	δ_{ex}	RMS	δ_{ex}	RMS
6^2	5.8×10^{-3}	8.9341×10^{-3}	1.7×10^{-2}	1.2324×10^{-3}
7^2	5.7×10^{-3}	1.9341×10^{-3}	1.0×10^{-2}	1.0561×10^{-3}
8^2	5.3×10^{-3}	7.9201×10^{-4}	8.9×10^{-3}	3.7213×10^{-3}
9^2	8.3×10^{-4}	3.2047×10^{-4}	6.3×10^{-3}	7.7001×10^{-4}
10^2	5.8×10^{-4}	2.6000×10^{-4}	2.3×10^{-3}	9.1540×10^{-4}
11^2	3.2×10^{-3}	3.9805×10^{-4}	9.3×10^{-4}	1.5170×10^{-4}
12^2	2.5×10^{-2}	1.2005×10^{-3}	5.3×10^{-3}	5.3072×10^{-3}

5 | Conclusion

A meshless local RBF method was proposed for solving one and two-dimensional FIEs. In the local RBF method, the approximate solution at stencil centers was expressed in terms of the given nodal values u(xj), which correspond to the n-nearest neighboring points. This allowed for the determination of the approximate function values at the nodal points without the need to calculate unknown coefficients λj. Numerical results demonstrated that the local RBF method outperformed the global RBF method, particularly in two-dimensional FIEs. This suggests that the local RBF method is more suitable for high-dimensional problems.

The effectiveness of the proposed method can be attributed to the following reasons:

I. The use of the strong form equation and collocation approach simplified the method.
II. By employing the localization approach, the matrix operations only required the inversion of small-sized matrices, resulting in a sparse final global matrix.

Based on these advantages, it is recommended to utilize the proposed method for tackling more complex and similar applied problems.

References

[1] Podlubny, I. (1999). Fractional differential equations, mathematics in science and engineering. In *Mathematics in science and engineering* (pp. 1–340). Academic press New York.

[2] Avazzadeh, Z., Hassani, H., Agarwal, P., Mehrabi, S., Ebadi, M. J., & Hosseini Asl, M. K. (2023). Optimal study on fractional fascioliasis disease model based on generalized Fibonacci polynomials. *Mathematical methods in the applied sciences*, *46*(8), 9332–9350. DOI:10.1002/mma.9057

[3] Avazzadeh, Z., Hassani, H., Ebadi, M. J., Agarwal, P., Poursadeghfard, M., & Naraghirad, E. (2023). Optimal approximation of fractional order brain tumor model using generalized laguerre polynomials. *Iranian journal of science*, *47*(2), 501–513. DOI:10.1007/s40995-022-01388-1

[4] Jafari, H., Malinowski, M. T., & Ebadi, M. J. (2021). Fuzzy stochastic differential equations driven by fractional Brownian motion. *Advances in difference equations*, *2021*(1), 1–17.

[5] Radmanesh, M., & Ebadi, M. J. (2020). A local mesh-less collocation method for solving a class of time-dependent fractional integral equations: 2D fractional evolution equation. *Engineering analysis with boundary elements*, *113*, 372–381. DOI:10.1016/j.enganabound.2020.01.017

[6] Abdollahi, Z., Mohseni Moghadam, M., Saeedi, H., & Ebadi, M. J. (2022). A computational approach for solving fractional Volterra integral equations based on two-dimensional Haar wavelet method. *International journal of computer mathematics*, *99*(7), 1488–1504.

[7] Avazzadeh, Z., Hassani, H., Agarwal, P., Mehrabi, S., Ebadi, M. J., & Dahaghin, M. S. (2023). An optimization method for studying fractional-order tuberculosis disease model via generalized Laguerre polynomials. *Soft computing*, *27*(14), 9519–9531. DOI:10.1007/s00500-023-08086-z

[8] Jafari, H., & Farahani, H. (2023). An approximate approach to fuzzy stochastic differential equations under sub-fractional Brownian motion. *Stochastics and dynamics*, 2350017. https://doi.org/10.1142/S021949372350017X

[9] Radmanesh, M., & Ebadi, M. J. (2022). A local meshless rbf method for solving fractional integral equations. *Sixth international conference on analysis and applied mathematics* (p. 154). ICAAM.

[10] Jafari, H., & Ebadi, M. J. (2022). *Expected value of supremum of some fractional gaussian processes* [presentation]. Sixth international conference on analysis and applied mathematics (Vol. 156). http://icaam-online.org/Abstractbook.pdf#page=156

[11] Farahani, H., Ebadi, M. J., & Jafari, H. (2019). Finding inverse of a fuzzy matrix using eigen value method. *International journal of innovative technology and exploring engineering*, *9*(2), 3030–3037. DOI:10.35940/ijitee.b6295.129219

[12] Avazzadeh, Z., Hassani, H., Eshkaftaki, A. B., Ebadi, M. J., Asl, M. K. H., Agarwal, P., … Dahaghin, M. S. (2023). An Efficient algorithm for solving the fractional hepatitis b treatment model using generalized bessel polynomial. *Iranian journal of science*, *47*(5–6), 1649–1664. DOI:10.1007/s40995-023-01521-8

[13] Hassani, H., Avazzadeh, Z., Agarwal, P., Mehrabi, S., Ebadi, M. J., Dahaghin, M. S., & Naraghirad, E. (2023). A study on fractional tumor-immune interaction model related to lung cancer via generalized Laguerre polynomials. *BMC medical research methodology*, *23*(1), 189. DOI:10.1186/s12874-023-02006-3

[14] Diethelm, K. (2010). *The analysis of fractional differential equations*. Springer.

[15] Cui, M. (2021). Finite difference schemes for the two-dimensional multi-term time-fractional diffusion equations with variable coefficients. *Computational and applied mathematics*, *40*(5), 167. DOI:10.1007/s40314-021-01551-1

[16] Shen, J., Tang, T., & Wang, L. L. (2011). *Spectral methods: algorithms, analysis and applications* (Vol. 41). Springer.

[17] Liu, G. R., & Karamanlidis, D. (2003). Mesh free methods: moving beyond the finite element method. *Applied mechanics reviews*, *56*(2), B17--B18.

[18] Buhmann, M. D. (2000). Radial basis functions. *Acta numerica*, *9*, 1–38. DOI:10.1017/S0962492900000015

[19] Kansa, E. J. (1990). Multiquadrics-A scattered data approximation scheme with applications to computational fluid-dynamics-I surface approximations and partial derivative estimates. *Computers and mathematics with applications*, *19*(8–9), 127–145. DOI:10.1016/0898-1221(90)90270-T

[20] Dehghan, M., & Mirzaei, D. (2008). The meshless local Petrov-Galerkin (MLPG) method for the generalized two-dimensional non-linear Schrödinger equation. *Engineering analysis with boundary elements*, *32*(9), 747–756. DOI:10.1016/j.enganabound.2007.11.005

[21] Wang, Y., Huang, J., & Li, H. (2023). A Numerical Approach for the System of Nonlinear Variable-order Fractional Volterra Integral Equations. *Numerical algorithms*, 1–23. DOI:10.1007/s11075-023-01630-w

[22] Wendland, H. (2004). *Scattered data approximation* (Vol. 17). Cambridge University Press.

[23] Oñate, E., Idelsohn, S., Zienkiewicz, O. C., & Taylor, R. L. (1996). A finite point method in computational mechanics: Applications to convective transport and fluid flow. *International journal for numerical methods in engineering*, *39*(22), 3839–3866.

[24] Assari, P., & Dehghan, M. (2017). A meshless discrete collocation method for the numerical solution of singular-logarithmic boundary integral equations utilizing radial basis functions. *Applied mathematics and computation*, *315*, 424–444. DOI:10.1016/j.amc.2017.07.073

[25] Sun, L., Chen, W., & Zhang, C. (2013). A new formulation of regularized meshless method applied to interior and exterior anisotropic potential problems. *Applied mathematical modelling*, *37*(12–13), 7452–7464.

[26] Yao, G., Tsai, C. H., & Chen, W. (2010). The comparison of three meshless methods using radial basis functions for solving fourth-order partial differential equations. *Engineering analysis with boundary elements*, *34*(7), 625–631. DOI:10.1016/j.enganabound.2010.03.004

[27] Shirzadi, A., Ling, L., & Abbasbandy, S. (2012). Meshless simulations of the two-dimensional fractional-time convection-diffusion-reaction equations. *Engineering analysis with boundary elements*, *36*(11), 1522–1527. DOI:10.1016/j.enganabound.2012.05.005

[28] Shirzadi, A., & Ling, L. (2013). Convergent overdetermined-RBF-MLPG for solving second order elliptic pdes. *Advances in applied mathematics and mechanics*, *5*(1), 78–89. DOI:10.4208/aamm.11-m11168

[29] Abbasbandy, S., & Shirzadi, A. (2011). MLPG method for two-dimensional diffusion equation with Neumann's and non-classical boundary conditions. *Applied numerical mathematics*, *61*(2), 170–180. DOI:10.1016/j.apnum.2010.09.002

[30] Shirzadi, A. (2014). Solving 2D reaction-diffusion equations with nonlocal boundary conditions by the RBF-MLPG method. *Computational mathematics and modeling*, *25*(4), 521–529. DOI:10.1007/s10598-014-9246-x

[31] Dehghan, M., & Mirzaei, D. (2009). Meshless local petrov-galerkin (MLPG) method for the unsteady magnetohydrodynamic (MHD) flow through pipe with arbitrary wall conductivity. *Applied numerical mathematics*, *59*(5), 1043–1058. DOI:10.1016/j.apnum.2008.05.001

[32] Shirzadi, A., & Takhtabnoos, F. (2016). A local meshless method for Cauchy problem of elliptic PDEs in annulus domains. *Inverse problems in science and engineering*, *24*(5), 729–743. DOI:10.1080/17415977.2015.1061521

[33] Lee, C. K., Liu, X., & Fan, S. C. (2003). Local multiquadric approximation for solving boundary value problems. *Computational mechanics*, *30*(5–6), 396–409. DOI:10.1007/s00466-003-0416-5

[34] Li, M., Chen, W., & Chen, C. S. (2013). The localized RBFs collocation methods for solving high dimensional PDEs. *Engineering analysis with boundary elements*, *37*(10), 1300–1304. DOI:10.1016/j.enganabound.2013.06.001

[35] Shirzadi, A., & Takhtabnoos, F. (2015). A local meshless collocation method for solving Landau-Lifschitz-Gilbert equation. *Engineering analysis with boundary elements*, *61*, 104–113. DOI:10.1016/j.enganabound.2015.07.010

[36] Takhtabnoos, F., & Shirzadi, A. (2016). A new implementation of the finite collocation method for time dependent PDEs. *Engineering analysis with boundary elements*, *63*, 114–124. DOI:10.1016/j.enganabound.2015.11.007

[37] Najafalizadeh, S., & Ezzati, R. (2016). Numerical methods for solving two-dimensional nonlinear integral equations of fractional order by using two-dimensional block pulse operational matrix. *Applied mathematics and computation*, *280*, 46–56. DOI:10.1016/j.amc.2015.12.042

[38] Abbas, S., & Benchohra, M. (2014). Fractional order integral equations of two independent variables. *Applied mathematics and computation*, *227*, 755–761. DOI:10.1016/j.amc.2013.10.086

[39] Yao, G. (2011). *Local radial basis function methods for solving partial differential equations*. The University of Southern Mississippi.

[40] Pandey, R. K., Singh, O. P., & Singh, V. K. (2009). Efficient algorithms to solve singular integral equations of Abel type. *Computers and mathematics with applications*, *57*(4), 664–676. DOI:10.1016/j.camwa.2008.10.085

[41] Lepik, Ü. (2009). Solving fractional integral equations by the Haar wavelet method. *Applied mathematics and computation*, *214*(2), 468–478. DOI:10.1016/j.amc.2009.04.015